Cu^{II} coordination polymers derived from bis-pyridyl-bis-urea ligands: synthesis, selective anion separation and metallogelation

N. N. Adarsh[1], D. Krishna Kumar[2] and Parthasarathi Dastidar[1,*]

[1]Department of Organic Chemistry, Indian Association for the Cultivation of Science, Jadavpur, 2A&2B Raja S.C. Mullick Road, Kolkata 700 032, India
[2]Present address: Department of Chemistry, Imperial College, London, SW7 ZAZ, UK

The reaction of $CuSO_4 \cdot 5H_2O$ with a series of bis-pyridyl-bis-urea ligands equipped with aliphatic backbone such as *N*,*N*′-bis-(3-pyridyl)ethylene-bis-urea L1, *N*,*N*′-bis-(3-pyridyl)propylene-bis-urea L2 and *N*,*N*′-bis-(3-pyridyl)butylene-bis-urea L3 in aqueous solution (metal : ligand ratio = 1 : 2) resulted in four coordination polymers (CPs): $[\{Cu(H_2O)_2(SO_4)(L1)_{1.5}\}\cdot 9.5H_2O]_\infty$ (1), $[\{Cu(H_2O)_3(SO_4)(L2)\}\cdot(H_2O)(EtOH)]_\infty$ (2a), $[Cu(H_2O)_4(SO_4)(L2)_2]_\infty$ (2b) and $[\{Cu(1)(H_2O)_2(SO_4)_1(\mu\text{-}L3)_3Cu(2)(H_2O)_2(SO_4)_1(\mu\text{-}L3)_3\}\cdot 20.5H_2O]_\infty$ (3). Except 2b which was concomitantly formed with 2a, all the CPs were characterized by single crystal X-ray diffraction. X-ray powder diffraction, FTIR and elemental analysis data confirmed that all the ligands were able to separate selectively, an important anion SO_4^{2-} from a complex mixture of oxo-anions such as SO_4^{2-}, NO_3^-, ClO_4^- and $CF_3SO_3^-$ in the form of the corresponding CPs. L3 formed a gel when it reacted with $CuSO_4$ in DMSO/H_2O and DMF/H_2O mixture with a minimum gelator concentration of 8–10 wt%, and the gel was characterized by tube inversion test, field emission scanning electron microscopy and rheology.

Keywords: Coordination polymers, hydrogen-bonding, metallogels, selective anion separation.

Introduction

COORDINATION compounds[1] such as coordination polymers (CPs) and coordination complexes formed via spontaneous self-assembly process of organic linkers (ligands) and metal centres (metal ions) are attractive in supramolecular chemistry and materials science because of their various potential applications[2]. Their ease of synthesis combined with the opportunity of isolating highly pure crystalline products that are amenable to detailed single crystal X-ray structural characterization to achieve need-based tuning of the final supramolecular structures make this class of functional materials more attractive.

Selective separation of anion from a complex mixture of anions via *in situ* crystallization of coordination compounds is one of the current interests[3], and is highly relevant to environmental issues[4]. In this technique, an organic ligand and metal salts having various counter anions are allowed to crystallize together. Ligands having multiple hydrogen-bonding functionalities such as amide, urea, etc. may attract anions via hydrogen bonding[5]. Separation of SO_4^{2-} from an aqueous solution containing a complex mixture of anions, including other oxo-anions such as NO_3^-, is an important issue in cleaning up radioactive waste tanks[4]. Since urea functionality can form a stable hydrogen-bonded structure with SO_4^{2-} anion resulting in the so-called urea–sulphate supramolecular synthon[6] (Scheme 1), ligands having urea moiety have been exploited to recognize/bind/separate SO_4^{2-} anion using *in situ* crystallization of coordination compounds[7].

Very recently, we have demonstrated that a Borromean[8] weave CP sustained by urea–sulphate synthon is able to separate SO_4^{2-} anion from a complex mixture of anions (SO_4^{2-}, NO_3^-, ClO_4^- and CF_3COO^-)[9]. We have also exploited urea–sulphate synthon to generate a porous self-assembly of nanorods based on a simple CP[7].

Another intriguing property of metal–organic compounds is their ability to form supramolecular gels with various solvents[10]. The so-called metallogel[11] (in order to emphasize the role of metal–ligand coordination in gelation) is believed to be formed due to the immobilization of the solvent molecules within the gel network formed via metal–ligand coordination and other non-bonded interactions such as hydrogen bonding, π–π stacking, van der Waals interactions, etc. Such materials (metallogels) display various potential applications such as catalysis, sensing, photophysics, magnetic materials[11], etc.

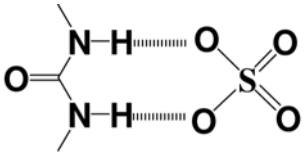

Scheme 1. Urea–sulphate supramolecular synthon.

*For correspondence. (e-mail: ocpd@iacs.res.in)

As a part of our ongoing research efforts[7,9,12] to generate intriguing coordination compounds, we have decided to exploit an analogous series of bis-pyridyl-bis-urea ligands, namely *N*,*N*′-bis-(3-pyridyl)ethylene-bis-urea (**L1**), *N*,*N*′-bis-(3-pyridyl)propylene-bis-urea (**L2**) and *N*,*N*′-bis-(3-pyridyl)butylene-bis-urea (**L3**) (Scheme 2), with the aim of producing CPs capable of displaying multiple properties such as anion separation and metallogelation.

The bis-urea moieties in these ligands are capable of forming hydrogen-bonding interactions with SO_4^{2-}, thereby facilitating SO_4^{2-} separation in the form of CPs. In fact, **L1** has been shown to separate SO_4^{2-} anion selectively in the form of Ni(II)[13] and Zn(II)[12] CPs. This hydrogen-bonding functionality, namely bis-urea is also expected to play an important role in forming a supramolecular network under suitable conditions in the corresponding coordination compounds capable of forming metallogels. With this background, we reacted **L1**–**L3** with $CuSO_4$ in 1 : 2 (metal : ligand) molar ratio separately and studied the effect of chain length of the ligand backbone on the structure, anion separation and metallogelation properties of the corresponding coordination compounds.

Experimental section

Materials and method

All chemicals were commercially available (Aldrich) and used without further purification. **L1** was previously reported by us[12], and the synthesis of **L2** and **L3** was reported by Byrne *et al.*[14]. However, we have followed a different method to synthesize **L2** and **L3**, as given in the synthesis section. The elemental analyses were carried out using a Perkin–Elmer 2400 Series-II CHN analyser. Fourier transform infrared (FTIR) spectra were recorded using Perkin–Elmer Spectrum GX and thermogravimetric analysis (TGA) was performed on a SDT Q Series 600 Universal VA.2E TA instrument. X-ray powder diffraction (XRPD) patterns were recorded on a Bruker AXS D8 Advance Powder (CuKα_1 radiation, λ = 1.5406 Å) X-ray diffractometer. Electron microscopic studies were made using a JEOL, JMS-6700F field emission scanning electron microscope (FESEM). Rheology experiments were performed in SDT Q Series Advanced Rheometer AR 2000.

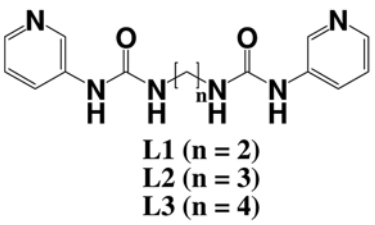

Scheme 2. Various ligands studied herein.

Synthesis

*Synthesis of ligands **L1**–**L3***

*N,N′-bis-(3-pyridyl)ethylene-bis-urea **L1**:* Synthesis and physico-chemical characterization has been previously reported by us[12].

*N,N′-bis-(3-pyridyl)propylene-bis-urea **L2**:* To a stirring solution of 3-aminopyridine (686 mg, 7.29 mmol) and triethylamine (3 ml) in 100 ml of anhydrous dichloromethane (DCM) at ice-cold temperature under an inert atmosphere was added triphosgene (900 mg, 3.030 mmol) and stirred for 20 min. A solution of 1,3-diaminopropane (270 mg, 3.65 mmol) in 50 ml of dry DCM was then added dropwise to the stirred solution that resulted in turbidity. A thick, white precipitate was obtained after half an hour of stirring; the stirring was continued for another 24 h at room temperature. The white precipitate was then filtered, washed with DCM, air-dried and treated with a 5% $NaHCO_3$ solution. The resultant solid was then filtered, washed with distilled water and air-dried. The crude product thus obtained was then dissolved in methanol, and further addition of distilled water gave **L2** as a gelly precipitate, which was then filtered and air-dried (800 mg, 70% yield). m.p. 196°C. Analysis calculated for $C_{15}H_{18}N_6O_2$ (%): C, 57.31; H, 5.77; N, 26.74. Found: C, 57.82; H, 5.72; N, 26.32. ^{1}H NMR (300 MHz, DMSO-d_6): δ = 8.68 (2H, s, N–H), 8.51 (2H, s, Py–H), 8.08–8.07 (2H, d, J = 3.0 Hz, Py–H), 7.87–7.84 (2H, d, J = 9.0 Hz, Py–H), 7.24-7.19 (2H, dd, J = 3.0, 9.0 Hz, Py–H), 6.34–6.30 (2H, t, J = 6.0 Hz, urea N–H), 3.15–3.10 (4H, q, J = 6.0 Hz, –CH_2–), 1.59–1.55 (2H, m, –CH_2–) ppm. ^{13}C NMR (300 MHz, DMSO-d_6): 155.8 (C), 142.6 (CH), 140.1 (CH), 137.8 (C), 125.0 (CH), 124.0 (CH), 37.2 (CH_2), 31.1 (CH_2) ppm. FTIR (KBr pellet): 3323 (s, urea ν N–H), 3146w, 3037 (m, aromatic ν C–H), 2814w, 1699s, 1660 (s, urea ν C=O), 1600 (s, urea δ N–H), 1587s, 1552s, 1523s, 1477s, 1442w, 1419s, 1373w, 1332m, 1288s, 1267s, 1249m, 1228m, 1124m, 1107w, 1055w, 1024m, 981w, 929w, 858m, 802s, 759m, 704w, 642w, 624w, 526w cm^{-1}. High resolution mass spectra (HRMS) calculated for $C_{15}H_{18}N_6O_2$ $[M + H]^+$: 315.15; found: 315.23.

*N,N′-bis-(3-pyridyl)butylene-bis-urea **L3**:* **L3** was synthesized using the method described above. (750 mg, 63% yield) Anal. calcd. for $C_{16}H_{20}N_6O_2$ (%): C, 58.52; H, 6.14; N, 25.59. Found: C, 58.82; H, 6.12; N, 25.44. ^{1}H NMR (300 MHz, DMSO-d_6): δ = 8.58 (2H, s, N–H), 8.50 (2H, s, Py–H), 8.08 (2H, s, Py–H), 7.87–7.84 (2H, d, J = 6.0 Hz, Py–H), 7.23–7.20 (2H, dd, J = 6.0, 9.0 Hz, Py–H), 6.29–6.28 (4H, t, J = 6.0 Hz, urea N–H), 3.09 (4H, s, –CH_2–), 1.47 (4H, s, –CH_2–) ppm. ^{13}C NMR (300 MHz, DMSO-d_6): 155.1 (C), 141.9 (CH), 139.4 (CH), 137.2 (C), 124.4 (CH), 123.4 (CH), 39.5 (CH_2),

27.3 (CH_2) ppm. FTIR (KBr pellet): 3324 (s, urea ν N–H), 3142w, 3034 (m, aromatic ν C–H), 2810w, 1694s, 1643 (s, urea ν C=O), 1556 (s, urea δ N–H), 1588s, 1550s, 1522s, 1470s, 1444w, 1421s, 1372w, 1330m, 1280s, 1237s, 1241m, 1222m, 1120m, 1101w, 1051w, 1020m, 973w, 934w, 877m, 811s, 754m, 702w, 621w cm^{-1}. HRMS calculated for $C_{15}H_{18}N_6O_2$ $[M + H]^+$: 329.17; found: 329.23.

*Synthesis of coordination polymers **1**–**3***

*$[\{Cu(H_2O)_2(SO_4)(\mu$-**L1**$)1.5\}\cdot 9.5H_2O]_\infty$* ***1***: **1** was synthesized by layering a methanolic solution of **L1** (60 mg, 0.2 mmol) over an aqueous ethanolic solution of $CuSO_4\cdot 5H_2O$ (25 mg, 0.1 mmol). After 1 week, green-coloured, plate-shaped crystals were obtained. Yield: 50 mg, 61% Anal. data calcd. for $C_{21}H_{28}N_9O_9CuS\cdot 6H_2O$: C, 33.44; H, 5.35; N, 16.71. Found: C, 33.34; H, 5.26; N, 16.85. FTIR (KBr, cm^{-1}): 3315 (sb, water ν O–H), 3130 (sb, urea ν N–H), 3086 (sb, aromatic ν C–H), 1685 (sb, urea ν C=O), 1614 m, 1591 (s, urea δ N–H), 1560s, 1481s, 1429s, 1330m, 1298m, 1269s, 1228s, 1195m, 1114 (s, sulphate ν S=O), 1051s, 998w, 879m, 804m, 696s, 651m, 609m.

*$[\{Cu(H_2O)_3(SO_4)(\mu$-**L2**$)\}\cdot(H_2O)(EtOH)]_\infty$* ***2a*** *and structurally unknown $[Cu(H_2O)_4(SO_4)($**L2**$)_2]_\infty$* ***2b***: Green-coloured, chunky crystals of coordination polymer **2a** and structurally unknown dark-blue microcrystals of **2b** were concomitantly formed after 4 days when an methanolic solution of **L2** (60 mg, 0.19 mmol) was layered over an aqueous ethanolic solution of $CuSO_4\cdot 5H_2O$ (24 mg, 0.095 mmol).

2a – Yield: 23 mg 41% Anal. data calcd. for $C_{15}H_{24}N_6O_9CuS\cdot EtOH$: C, 35.57; H, 5.27; N, 14.64. Found: C, 35.04; H, 5.02; N, 14.20. FTIR (KBr, cm^{-1}): 3350 (sb, water ν O–H), 3300 (sb, urea ν N–H), 3090 (sb, aromatic ν C–H), 1701s, 1664 (sb, urea ν C=O), 1593 (s, urea δ N–H), 1552s, 1523s, 1483s, 1427s, 1413s, 1338m, 1305s, 1274s, 1238s, 1130 (s, sulphate ν S=O), 1103s, 1051s, 968s, 922w, 819m, 798m, 692s, 617m.

2b – Yield: 40 mg Anal. data calcd. for $C_{30}H_{44}N_{12}O_{12}CuS$: C, 41.88; H, 5.15; N, 19.54. Found: C, 41.98; H, 4.67; N, 19.21. FTIR (KBr, cm^{-1}): 3269 (sb, urea ν N–H), 3070 (sb, aromatic ν C–H), 2968m, 2864m, 1681 (sb, urea ν C=O), 1552 (s, urea ν N–H), 1483s, 1425s, 1332m, 1300s, 1271s, 1230s, 1099 (s, sulphate ν S=O), 1062s, 1024w, 902w, 881w, 810s, 700s, 613m.

*$[\{Cu(1)(H_2O)_2(SO_4)_1(\mu$-**L3**$)_3Cu(2)(H_2O)_2(SO_4)_1(\mu$-**L3**$)_3\}\cdot 20.5H_2O]_\infty$* ***3***: **3** was synthesized by layering a methanolic solution of **L3** (60 mg, 0.18 mmol) over an aqueous ethanolic solution of $CuSO_4\cdot 5H_2O$ (22.4 mg, 0.09 mmol). After 4 days, green-coloured plate-shaped crystals were obtained. Yield: 60 mg, 38% Anal. data calcd. for $C_{48}H_{68}N_{18}O_{18}Cu_2S_2\cdot 19H_2O$: C, 33.54; H, 6.22; N, 14.67. Found: C, 33.13; H, 5.97; N, 14.01. FTIR (KBr, cm^{-1}): 3346 (sb, water ν O–H), 3267 (sb, urea ν N–H), 3086 (sb, aromatic ν C–H), 1672 (sb, urea ν C=O), 1608 (s, urea δ N–H), 1556s, 1492s, 1458m, 1415m, 1332m, 1327m, 1286m, 1251m, 1234m, 1078 (s, sulphate ν S=O), 1031m, 815w, 763w, 702m.

X-ray crystallography

X-ray single-crystal data were collected using MoKα (λ = 0.7107 Å) radiation on a SMART APEX diffractometer equipped with CCD area detector. Data collection, data reduction and structure solution/refinement were carried out using the software package of SMART APEX. All the structures were solved by direct method and refined in a routine manner. In most of the cases, nonhydrogen atoms were treated anisotropically. Whenever possible, the hydrogen atoms were located on a difference Fourier map and refined. In other cases, the hydrogen atoms were geometrically fixed. CCDC no. 790325–790327 contains the supplementary crystallographic data for this article. These data can be obtained free of charge via www.ccdc.cam.ac.uk/conts/retrieving.html (or from the Cambridge Crystallographic Data Centre, 12 Union Road, Cambridge CB21EZ, UK; fax: (+44) 1223-336-033; or deposit@ccdc.cam.ac.uk).

Results and discussion

Synthesis

The ligands **L1**–**L3** were reacted with $CuSO_4\cdot 5H_2O$ in a 2 : 1 (ligand : metal) molar ratio by layering method; a methanolic solution of the ligand was layered over aqueous ethanolic solution of $CuSO_4\cdot 5H_2O$. After keeping the reaction mixture at ambient condition for about 1 week, single crystals suitable for X-ray diffraction were obtained (see experimental section). Table 1 contains the crystallographic data. Crystal structure analyses revealed that the crystals obtained have the following chemical formulae – $[\{Cu(H_2O)_2(SO_4)(\mu$-**L1**$)_{1.5}\}\cdot 9.5H_2O]_\infty$ **1**, $[\{Cu(H_2O)_3(SO_4)(\mu$-**L2**$)\}\cdot(H_2O)(EtOH)]_\infty$ **2a** and the structurally unknown $[Cu(H_2O)_4(SO_4)($**L2**$)_2]_\infty$ **2b** (**2a** and **2b** are concomitantly formed; chemical formula of **2b** is based on elemental analysis and FTIR), and $[\{Cu(1)(H_2O)_2(SO_4)_1(\mu$-**L3**$)_3Cu(2)(H_2O)_2(SO_4)_1(\mu$-**L3**$)_3\}\cdot 20.5H_2O]_\infty$ **3**.

Single-crystal structures

*Coordination polymer $[\{Cu(H_2O)_2(SO_4)(\mu$-**L1**$)_{1.5}\}\cdot 9.5H_2O]_\infty$* ***1:*** Crystals of **1** belonged to the centrosymmetric monoclinic space group *P*2/*c*. The asymmetric unit contained one metal centre, Cu^{II}, one and a half molecules of **L1** (both crystallographically independent), a

Table 1. Crystal data

Crystal data	**1a**	**2a**	**3***
Empirical formula	$C_{21}H_{45}CuN_9O_{18.50}S$	$C_{17}H_{32}CuN_6O_{11}S$	$C_{48}H_{109}Cu_2N_{18}O_{38.50}S_2$
Formula weight	815.26	592.09	1745.73
Crystal size (mm)	0.28 × 0.19 × 0.12	0.22 × 0.16 × 0.08	0.24 × 0.12 × 0.06
Crystal system	Monoclinic	Monoclinic	Triclinic
Space group	$P2/c$	$P2_1$	$P1$
a (Å)	17.7573(14)	6.5512(2)	12.042(3)
b (Å)	12.0093(9)	19.3273(6)	17.455(4)
c (Å)	20.5836(13)	9.6400(3)	22.271(5)
α (°)			112.517(7)
β (°)	119.797(5)	98.0370(10)	91.705(9)
γ (°)			90.343(7)
Volume (Å^3)	3809.2(5)	1208.60(6)	4321.6(18)
Z	4	2	2
$D_{calc.}$ (g/cm^3)	1.422	1.627	1.342
F(000)	1708	618	1842
μ MoKα (mm^{-1})	0.710	1.060	0.632
Temperature (K)	298(2)	298(2)	298(2)
Range of h, k, l	–21/19, –13/14, –17/24	–7/7, –22/22, –11/11	–13/13, –19/20, –25/25
θ min/max	1.32/25.00	2.11/25.00	0.99/24.52
Reflections collected/unique/observed	18846/6702/4335	11427/3833/3729	37606/13250/7890
Data/restraints/parameters	6702/0/388	3833/9/359	13250/0/876
Goodness-of-fit on F^2	0.999	1.050	1.241
Final R indices [$I > 2\sigma(I)$]	R_1 = 0.0752	R_1 = 0.0236	R_1 = 0.1447
	wR_2 = 0.1894	wR_2 = 0.0601	wR_2 = 0.3672
R indices (all data)	R_1 = 0.1125	R_1 = 0.0245	R_1 = 0.1837
	wR_2 = 0.2057	wR_2 = 0.0608	wR_2 = 0.3917

*R_1 of **3** is reasonably high due to poor quality of the crystal [R(int) = 0.0933].

sulphate anion (coordinated to Cu^{II}), two metal-bound water molecules, two lattice-included water molecules and some unaccounted electron densities (302 e/Å^3 per unit cell), presumably coming from disordered solvents. The central C–C bond of one of the crystallographically independent ligands was positioned at the twofold symmetry axis and as a result, only half of the ligand was located in the asymmetric unit. The two crystallographically independent ligands displayed different conformations and consequently ligating topologies; whereas the half-occupied ligand displayed *syn–syn–syn* conformation, the fully occupied ligand showed *syn–anti–syn* conformation resulting in angular and linear ligating topologies respectively. Interestingly, the central C–C bond in both the cases, adopted energetically favoured staggered conformation; the free rotation around $C_{ethylene}$–N_{urea} bond was responsible for these two conformations. The free ligand structure reported by us[12] and also by others[13] displayed *anti–anti–anti* conformation. In the crystal structure of **1**, the sulphate anion coordinated to the Cu^{II} metal centre acted as a monodentate ligand. The metal centre displayed a slightly distorted octahedral geometry [∠N–Cu–N = 86.71(17)–92.09(17)°; ∠N–Cu–O = 87.68(16)–93.50(16)°; ∠O–Cu–O = 87.50(14)°]; the equatorial positions were occupied by the N atoms of **L1** and O atom of sulphate and the apical positions were coordinated by the water molecules. The crystallographically independent ligand **L1** displaying linear ligating topology formed 1D coordination polymeric chain via extended metal–ligand coordination; such chains arranged in parallel fashion were further bridged by the other crystallographically independent ligand **L1** having angular ligating topology displaying an overall 1D zigzag ladder topology (Figure 1). The metal-bound sulphate anion was found to be involved in intramolecular hydrogen-bonding interactions with the urea functionality of the ligand and metal-bound water [N···O = 2.824(6)–3.052(6)Å; ∠N–H···O = 153.6–160.8°; O···O = 2.701(5)Å]; it also formed intermolecular hydrogenbond with the urea moiety of the adjacent 1D chains [N···O = 2.840(6)–2.966(6)Å; ∠N–H···O = 150.4–154.4°], resulting in an overall 3D hydrogen-bonded network. The lattice-included water molecules were located within the groove of the 1D zigzag ladder and were sustained by hydrogen bonding among themselves [O···O = 2.845(9)Å], with urea carbonyl [O···O = 2.765(6)–2.897(9)Å] and with metal-bound water [O···O = 2.751(6)–2.781(8)Å].

*Coordination polymer [{Cu(H$_2$O)$_3$(SO$_4$)(μ-**L2**)}·(H$_2$O)(EtOH)]$_\infty$ **2a**:* CP **2a** was crystallized in the noncentrosymmetric monoclinic $P2_1$ space group. The asymmetric unit contained one metal centre, Cu^{II}, one molecule of **L2**, one sulphate anion, three metal-bound water molecules and two lattice-included solvent molecules, namely ethanol and water. The metal centre displayed a slightly distorted octahedral geometry [∠N–Cu–N = 92.00(9)°;

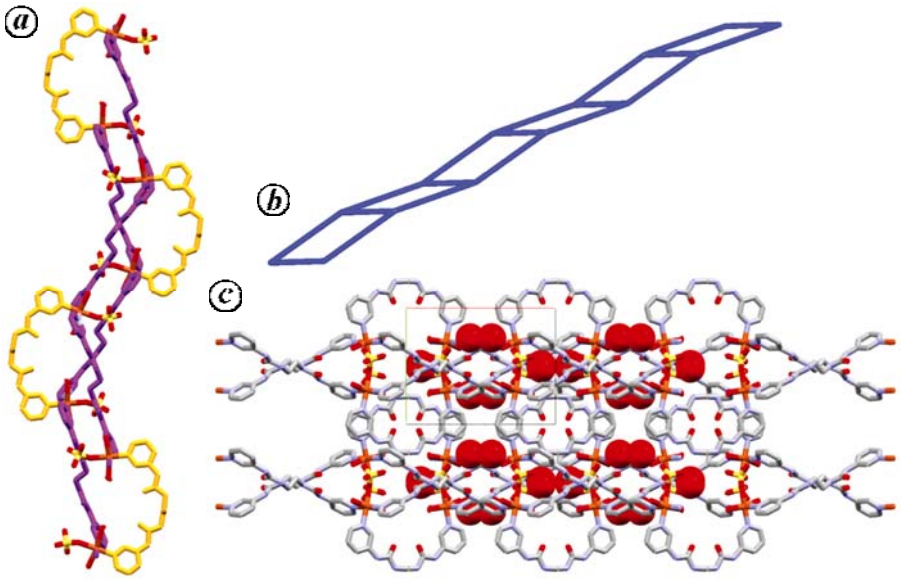

Figure 1. Crystal structure of **1**. ***a***, One-dimensional ladder type coordination polymer; ***b***, TOPOS[17] view of the one-dimensional ladder, and ***c***, Trapped lattice-included water molecules (red, space-fill model) inside the network involving various hydrogen-bonding interactions.

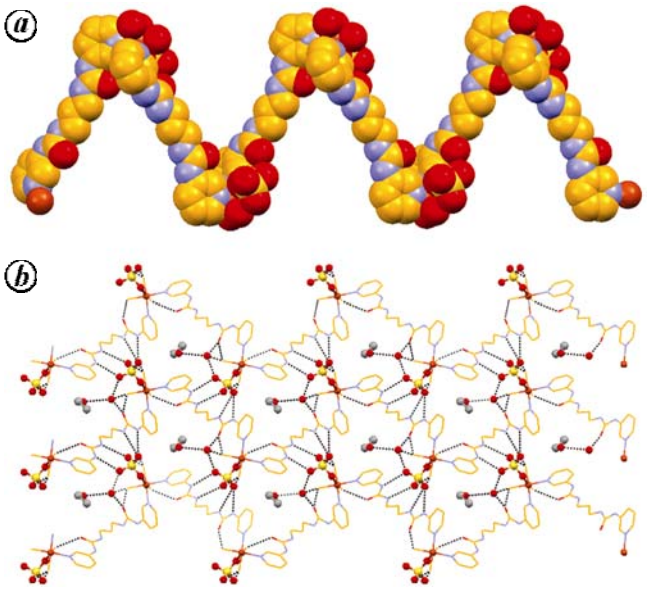

Figure 2. Crystal structure of **2a**. ***a***, One-dimensional zigzag coordination polymer and ***b***, Lattice-included water and ethanol displaying various hydrogen-bonding interactions.

∠N–Cu–O = 88.84(8)–95.91(8)°; ∠O–Cu–O = 88.95(8)–89.61(8)°]; the equatorial positions were occupied by the N atoms of **L2** and O atoms of water molecules, and the apical positions were coordinated by the water molecule and counter anion sulphate. In the crystal structure, **L2** showed *syn–syn–syn* conformation with the central propylene backbone displaying staggered conformation (see Scheme S2, supplementary material). Interestingly, the free ligand structure reported by Byrne *et al.*[14] displayed *syn–anti–syn* conformation. The sulphate anion coordinated to the Cu^{II} metal centre acted as a monodentate ligand. The extended coordination of **L2** in *syn–syn–syn* conformation led to the formation of 1D zigzag coordination polymer (Figure 2). The chains were further packed in parallel fashion displaying herringbone packing mode, further sustained by intermolecular hydrogen bonding involving the metal-bound sulphate anion, urea moieties of **L2** of the neighbouring chains [N···O = 2.978(3)–3.057(3)Å; ∠N–H···O = 149.8–151.4°], the metal-bound water [O···O = 2.642(3)–2.693(3)Å; ∠O–H···O = 159(4)–167(4)°] and the lattice-included water [O···O = 2.728(3)Å; ∠O–H···O = 162(4)°]. The lattice-included MeOH was found to be hydrogen bonded with the lattice-included water [O···O = 2.879(4) Å; ∠O–H···O = 164.1°].

Coordination polymer $[\{Cu(1)(H_2O)_2(SO_4)_1(\mu\text{-}\mathbf{L3})_3Cu(2)(H_2O)_2(SO_4)_1(\mu\text{-}\mathbf{L3})_3\}\cdot 20.5H_2O]_\infty$ ***3:*** Green-coloured, plate-shaped crystals of CP **3** were crystallized in the centrosymmetric triclinic $P\bar{1}$ space group. The asymmetric unit contained two crystallographically independent Cu^{II} metal centres, three crystallographically independent ligand molecules of **L3**, two sulphate anions, four molecules of water (all coordinated to the Cu^{II} metal centres), ten lattice-included water molecules and some unaccounted electron densities (211 e/Å^3 per unit cell), presumably coming from the disordered solvents. The Cu^{II} metal centres displayed a slightly distorted octahedral geometry [∠N–Cu(1)–N = 88.4(3)–90.9(3)°; ∠N–Cu(1)–O = 86.6(3)–93.8(3)°; ∠O–Cu(1)–O = 82.6(3)°; ∠N–Cu(2)–N = 88.7(3)–91.2(3)°; ∠N–Cu(2)–O = 86.0(3)–94.2(3)°; ∠O–Cu(2)–O = 78.8(3)–86.77(4)°]; the equatorial positions of both Cu(1) and Cu(2) were occupied by the N atoms of **L3** and O atom of sulphate anion, and the apical positions

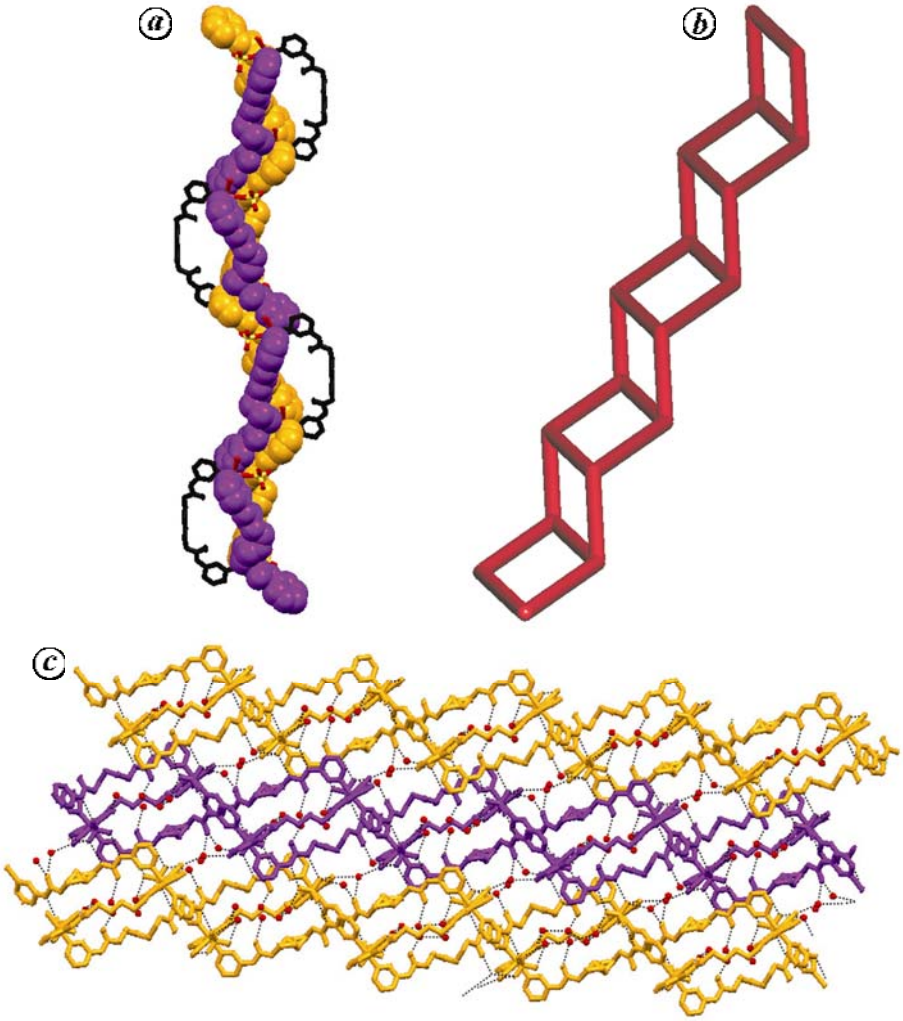

Figure 3. Crystal structure of **3**. ***a***, Side view of the one-dimensional staircase-type coordination polymer; ***b***, TOPOS[17] view of the staircase, and ***c***, Overall packing and lattice-included water molecules displaying various hydrogen-bonding interactions.

were coordinated by the water molecules. The central butyl moiety of one of the ligands appeared to be disordered and therefore, the conformation of the butyl moiety in this ligand was not clear; the butyl moiety in the other two ligands displayed all staggered and staggered–eclipsed–staggered conformation. The ligand displaying central butyl moiety in all staggered conformation adopted a *syn–syn–syn* conformation resulting in an angular ligating topology, whereas the other two ligands showed *syn–anti–syn* conformation resulting in linear ligating topology. The ligands having linear ligating topology formed 1D zigzag CP chains which were further arranged in parallel fashion bridged by the ligand displaying angular ligating topology, resulting in an overall distorted 1D ladder topology. Lattice-included water molecules were hydrogen bonded among themselves [O···O = 2.775(14)–2.892(12)Å], with metal-bound water [O···O = 2.664(12)–2.984(14)Å], with sulphate [2.809(11)–2.942(11)Å] and with urea carbonyl [2.691(13)–2.840(13)Å]. The sulphate anion was also extensively hydrogen bonded with urea functionality of the ligand [N···O = 2.823(12)–2.872(11)Å; ∠N–H···O = 139.2 173.9°] (Figure 3).

Thermogravimetric analysis

During refinement of the crystal structures of **1** and **3**, significant amount of smeared electron densities were located in the difference Fourier map. A SQUEEZE calculation[15] indicated the presence of 302 e/unit cell with a solvent accessible area volume of 1374.8 Å^3 in **1**. This may be attributed to 7.5 water molecules in the crystal lattice. TGA also supported this finding; a weight loss of 25.4% within the temperature range 27–179°C was attributed to 11.5 water molecules (2 coordinated + 2 ordered + 7.5 disordered lattice-included water molecules; calculated weight loss of 11.5 water = 25.32%) (see Figure S1, supplementary material).

TGA data of **2a** showed a weight loss of 18.1% within the temperature range 28–208°C, which was attributed to the loss of water and EtOH, one molecule each (calculated weight loss of 1 water + 1 EtOH = 19.9%) from the crystal lattice (see Figure S2, supplementary material). Single-crystal structure also supported this finding.

Disorderd electron densities were found in the final cycles of refinement in the crystal structure of **3**. These electron densities were attributed to the disordered water molecules and were squeezed out in the final cycles of refinement. SQUEEZE calculations showed the presence of 211 e/unit cell, with a solvent accessible area volume of 1299.1 Å^3. This may be attributed to 10.5 water molecules in the crystal lattice. TGA data also supported these results; a weight loss of 25.3% within the temperature range 28–198°C may be due to the weight loss of 24.5 water molecules (4 coordinated + 10 ordered + 10.5 disordered water molecules; see Figure S3, supplementary material). Thus, the TGA results corroborated well with the crystal structure of **1**, **2a** and **3**.

Anion separation

A systematic study of *in situ* crystallization experiments under non-competitive and competitive conditions was undertaken in all the three different metal–organic coordination networks **1**, **2a** and **3** in order to separate the sulphate anion from a complex mixture of anions. In the competitive condition, two types of experiment (conditions **I** and **II**) were carried out. In condition **I**, the corresponding ligand was reacted with a mixture of Cu^{II} salts [$CuSO_4$, $Cu(ClO_4)_2$, $Cu(NO_3)_2$ and $Cu(CF_3SO_3)_2$] in the molar ratio 2 : 1 (ligand : metal), whereas in condition **II** the reaction was performed using the ratio 2 : 1 : 2 [ligand : $CuSO_4$: {($Cu(ClO_4)_2$ + $Cu(NO_3)_2$ + $Cu(CF_3SO_3)_2$}]. In all cases, the experimental conditions (solvents, temperature, etc.) were kept unchanged as in the synthesis of **1**–**3** (see the supplementary material). In all the cases, the products obtained were thoroughly characterized by XRPD, FTIR and elemental analysis.

Green, plate-shaped crystals were obtained when **L1** was reacted with $CuSO_4$ and other metal salts in both the competitive conditions, i.e. conditions **I** and **II**. A strong and broad band at 1116 cm^{-1} in the crystalline products obtained in both the conditions was attributed to ν_{asymm} S–O of SO_4^{2-} anion. Interestingly, these FTIR spectra were almost identical with those obtained in non-competitive condition, indicating that CP **1** was crystallized out under competitive conditions.

This was further supported by both XRPD and elemental analysis data (Figure 4). Thus, it is clear from these experiments that **L1** is capable of separating SO_4^{2-} anion from a complex mixture of other oxo-anions in the form of CP **1**.

In the case of ligand **L2**, green-coloured chunky crystals along with some blue-coloured microcrystalline precipitate were obtained in all the conditions, i.e. non-competitive and competitive (conditions **I** and **II**). It was revealed from single-crystal X-ray diffraction experiment and other physico-chemical studies such as FTIR and elemental analysis that the green-coloured, Chunky crystals obtained in the noncompetitive condition were the CP **2a**, whereas the blue-coloured, microcrystalline precipitate was a structurally unknown CP **2b** having a plausible chemical formula $[Cu(H_2O)_4(SO_4)(\mathbf{L2})_2]_\infty$ **2b**. The fact that the FTIR spectra recorded for the various crystalline products in all the conditions were identical with each other in their respective category, clearly indicated that both **2a** and **2b** were being formed even in the competitive conditions; strong and broad bands at 1130 and 1099 cm^{-1} were attributed to ν_{asymm} S–O of the SO_4^{2-} anion present in **2a** and **2b** respectively (Figure 5).

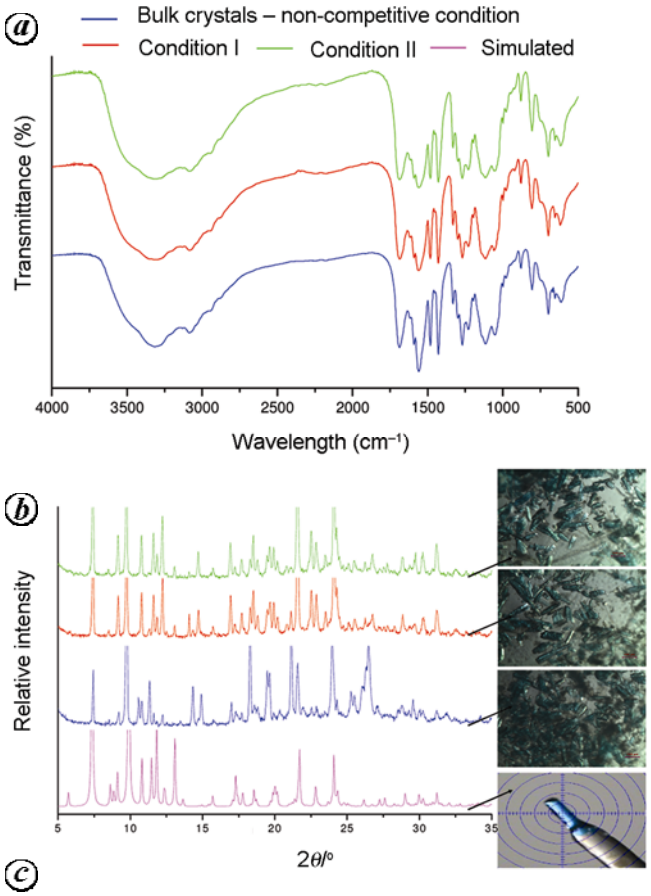

Non-competitive Condition	Condition I	Condition II
Calculated for $C_{21}H_{28}N_9O_9CuS{\cdot}6H_2O$ (%): C, 33.44; H, 5.35; N, 16.71 Found: C, 33.34; H, 5.26; N, 16.85	Calculated for $C_{21}H_{28}N_9O_9CuS{\cdot}5H_2O$ (%): C, 34.26; H, 5.20; N, 17.12 Found: C, 34.08; H, 5.01; N, 16.60	Calculated for $C_{21}H_{28}N_9O_9CuS{\cdot}6H_2O$ (%): C, 33.44; H, 5.35; N, 16.71 Found: C, 33.15; H, 5.72; N, 17.05

Figure 4. Fourier transform infrared (FTIR) spectroscopy (***a***), X-ray powder diffraction (PXRD) (***b***) and elemental analysis data (***c***) of **1** under various conditions. The right panel in (***b***) represents the optical micrographs of the corresponding crystals.

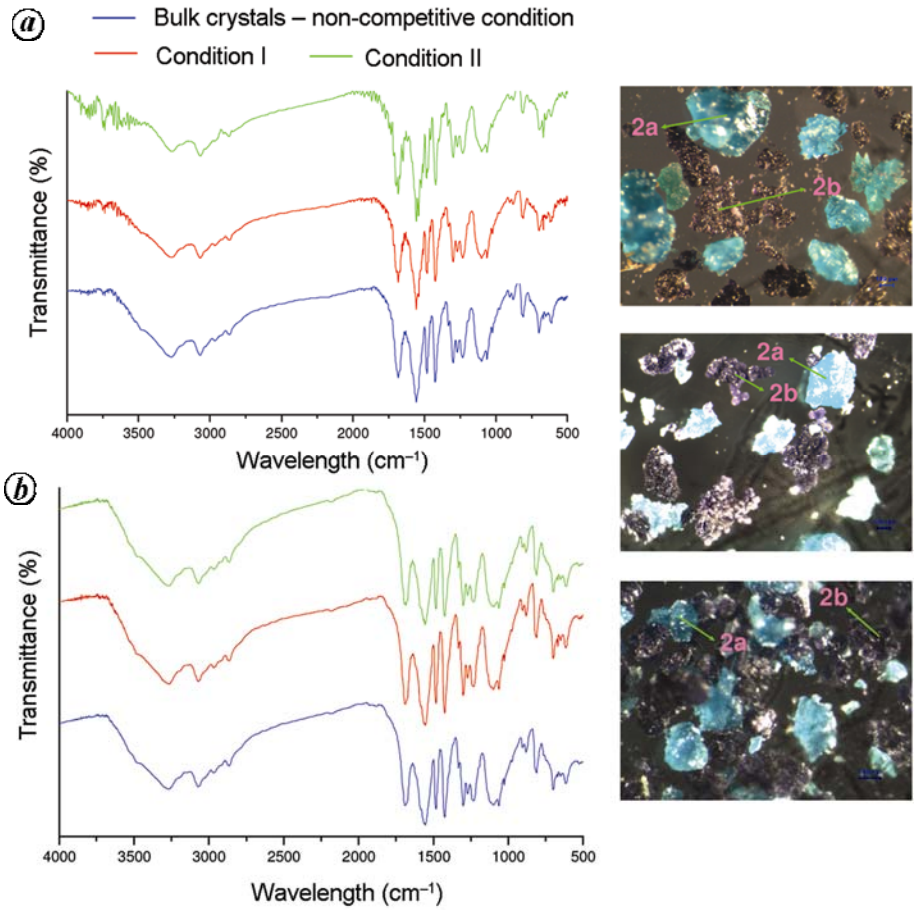

Figure 5. FTIR spectra comparison plot of crystals of **2a** (***a***) and **2b** (***b***) obtained at various conditions. Photographs of the crystals of **2a** and **2b** obtained at non-competitive condition, condition I and condition II respectively (from top to bottom).

It is interesting to note that XRPD patterns obtained for the green-coloured, chunky, bulk crystals of **2a** did not match with those obtained by simulating the single-crystal data of **2a**. This could be due to the loss of lattice-included water molecules during the grinding of the samples prepared from XRPD experiments. However, the corresponding XRPD patterns of the bulk samples obtained in the competitive conditions – both **I** and **II** – were almost superimposable with those obtained for bulk sample prepared under non-competitive condition. Elemental analysis data further supported these findings (Figure 6). Interestingly, the XRPD pattern of the bulk sample of **2b** matched well with that of the bulk samples obtained under competitive conditions (Figure 6); elemental analysis data also supported these findings (Figure 6). Therefore, **L2** is capable of separating SO_4^{2-} in the form of CPs **2a** and **2b** from a complex mixture of other oxo-anions.

Microscopic observation of the crystalline products obtained when **L3** was reacted with $CuSO_4$ and other metal salts under all the conditions (both non-competitive and competitive) revealed the formation of a similar kind of crystalline product in all the cases. FTIR spectra of these crystalline products were all found to be identical with each other, having a strong and broad band at 1087 cm^{-1}, which was assigned to be ν_{asymm} S–O of the SO_4^{2-} anion. It appears from the XRPD comparison plot that the simulated pattern of CP **3** did not match with the corresponding bulk samples obtained under non-competitive and competitive conditions. However, the experimental XRPD patterns of the bulk samples obtained under various conditions were identical with each other. This could be due to the loss of lattice-included water molecules that might have taken place during the grinding of the samples prepared for XRPD experiments. Elemental analysis data also supported this finding (Figure 7). Thus, **L3** is also capable of separating SO_4^{2-} anion from a complex mixture of other oxo-anions.

The flexibility of the aliphatic backbone as well as the free rotation of C–N_{urea} bond of the ligands appears to have played a crucial role in displaying various conformations resulting in both linear and angular ligating topology of the ligands in the CPs **1–3**. Although the metal : ligand molar ratio was kept fixed at 1 : 2 in all these reactions, various metal : ligand ratios such as 2 : 3

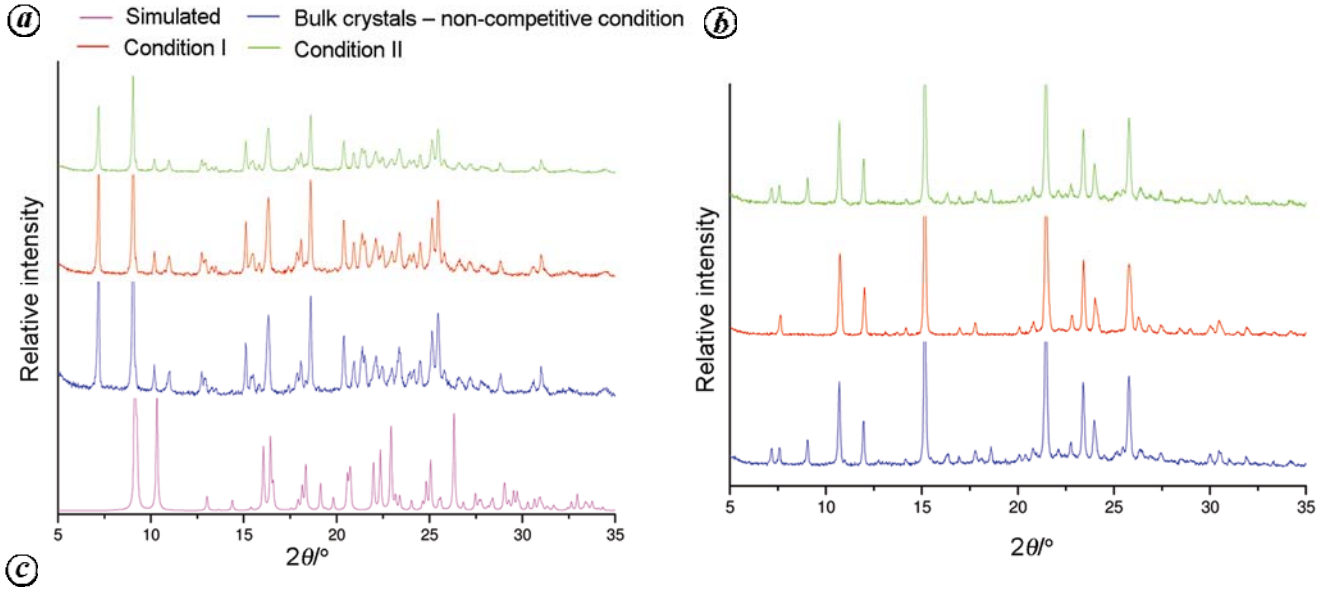

Compound	Non-competitive condition	Condition I	Condition II
2a	Calculated for $C_{15}H_{22}N_6O_8CuS{\cdot}H_2O.EtOH$ (%): C, 35.57; H, 5.27; N, 14.64 Found: C, 35.43; H, 4.92; N, 13.20	Calculated for $C_{15}H_{22}N_6O_8CuS{\cdot}H_2O.EtOH$ (%): C, 35.57; H, 5.27; N, 14.64 Found: C, 35.04; H, 5.02; N, 14.20	Calculated for $C_{15}H_{22}N_6O_8CuS{\cdot}H_2O.EtOH$ (%): C, 35.57; H, 5.27; N, 14.64 Found: C, 35.42; H, 5.14; N, 14.25
2b	Calculated for $C_{30}H_{44}N_{12}O_{12}CuS$ (%): C, 41.88; H, 5.15; N, 19.54 Found: C, 41.98; H, 4.67; N, 19.21	Calculated for $C_{30}H_{44}N_{12}O_{12}CuS$ (%): C, 41.88; H, 5.15; N, 19.54 Found: C, 41.78; H, 4.84; N, 19.12	Calculated for $C_{30}H_{44}N_{12}OCuS$ (%): C, 41.88; H, 5.15; N, 19.54 Found: C, 41.83; H, 4.81; N, 19.20

Figure 6. XRPD comparison plots of **2a** (***a***), **2b** (***b***) and elemental analysis data (***c***) under various conditions.

Table 2. Gelation data

Ligand	$CuSO_4{\cdot}5H_2O$	Metal : ligand	Aqueous solvent mixture used	Gel/precipitate	Minimum gelator concentration (wt%)
L1 (90 mg, 0.3 mmol)	75 mg, 0.3 mmol	1 : 1	DMSO–H_2O (0.75 + 0.75 = 1.5 ml)	Precipitate	
L1 (90 mg, 0.3 mmol)	75 mg, 0.3 mmol	1 : 1	DMF–H_2O (0.75 + 0.75 = 1.5 ml)	Precipitate	
L1 (90 mg, 0.3 mmol)	75 mg, 0.3 mmol	1 : 1	EG–H_2O (0.75 + 0.75 = 1.5 ml)	Precipitate	
L1 (90 mg, 0.3 mmol)	37.4 mg, 0.15 mmol	1 : 2	DMSO–H_2O (0.75 + 0.75 = 1.5 ml)	Precipitate	
L1 (90 mg, 0.3 mmol)	37.4 mg, 0.15 mmol	1 : 2	DMF–H_2O (0.75 + 0.75 = 1.5 ml)	Precipitate	
L1 (90 mg, 0.3 mmol)	37.4 mg, 0.15 mmol	1 : 2	EG–H_2O (0.75 + 0.75 = 1.5 ml)	Precipitate	
L2 (90 mg, 0.28 mmol)	70 mg, 0.28 mmol	1 : 1	DMSO–H_2O (0.75 + 0.75 = 1.5 ml)	Precipitate	
L2 (90 mg, 0.28 mmol)	70 mg, 0.28 mmol	1 : 1	DMF–H_2O (0.75 + 0.75 = 1.5 ml)	Precipitate	
L2 (90 mg, 0.28 mmol)	70 mg, 0.28 mmol	1 : 1	EG–H_2O (0.75 + 0.75 = 1.5 ml)	Precipitate	
L2 (90 mg, 0.28 mmol)	35 mg, 0.14 mmol	1 : 2	DMSO–H_2O (0.75 + 0.75 = 1.5 ml)	Precipitate	
L2 (90 mg, 0.28 mmol)	35 mg, 0.14 mmol	1 : 2	DMF–H_2O (0.75 + 0.75 = 1.5 ml)	Precipitate	
L2 (90 mg, 0.28 mmol)	35 mg, 0.14 mmol	1 : 2	EG–H_2O (0.75 + 0.75 = 1.5 ml)	Precipitate	
L3 (80 mg, 0.244 mmol) **G3C**	61 mg, 0.244 mmol	1 : 1	DMSO–H_2O (0.75 + 0.75 = 1.5 ml)	Weak gel	
L3 (80 mg, 0.244 mmol) **G3D**	61 mg, 0.244 mmol	1 : 1	DMF–H_2O (0.75 + 0.75 = 1.5 ml)	Weak gel	
L3 (80 mg, 0.244 mmol)	61 mg, 0.244 mmol	1 : 1	EG–H_2O (0.75 + 0.75 = 1.5 ml)	Precipitate	
L3 (80 mg, 0.244 mmol) **G3A**	30.4 mg, 0.122 mmol	1 : 2	DMSO–H_2O (0.75 + 0.75 = 1.5 ml)	Gel	7.3
L3 (80 mg, 0.244 mmol) **G3B**	30.4 mg, 0.122 mmol	1 : 2	DMF–H_2O (0.75 + 0.75 = 1.5 ml)	Gel	7.3
L3 (80 mg, 0.244 mmol)	30.4 mg, 0.122 mmol	1 : 2	EG–H_2O (0.75 + 0.75 = 1.5 ml)	Precipitate	

for **1** and **3** and 1 : 1 for **2a** were obtained. In addition to the nature of the metal centre and reaction conditions, this could also be due to the various conformations of the ligands adopted in the corresponding crystal structures in order to achieve the thermodynamically most stable form. As a result different network topologies such as 1D distorted ladder in **1** and **3** and 1D zigzag chain in **2a** were formed. High flexibility and the presence of bis-urea moiety in the ligands, tendency of SO_4^{2-} to coordinate to the Cu^{II} metal centre and its high hydrogen-bonding affinity towards the urea moiety are a few important reasons for all these ligands being so successful in separating SO_4^{2-} from a complex mixture of other oxo-anions. It may be mentioned here that SO_4^{2-} comes early in the Hofmeister

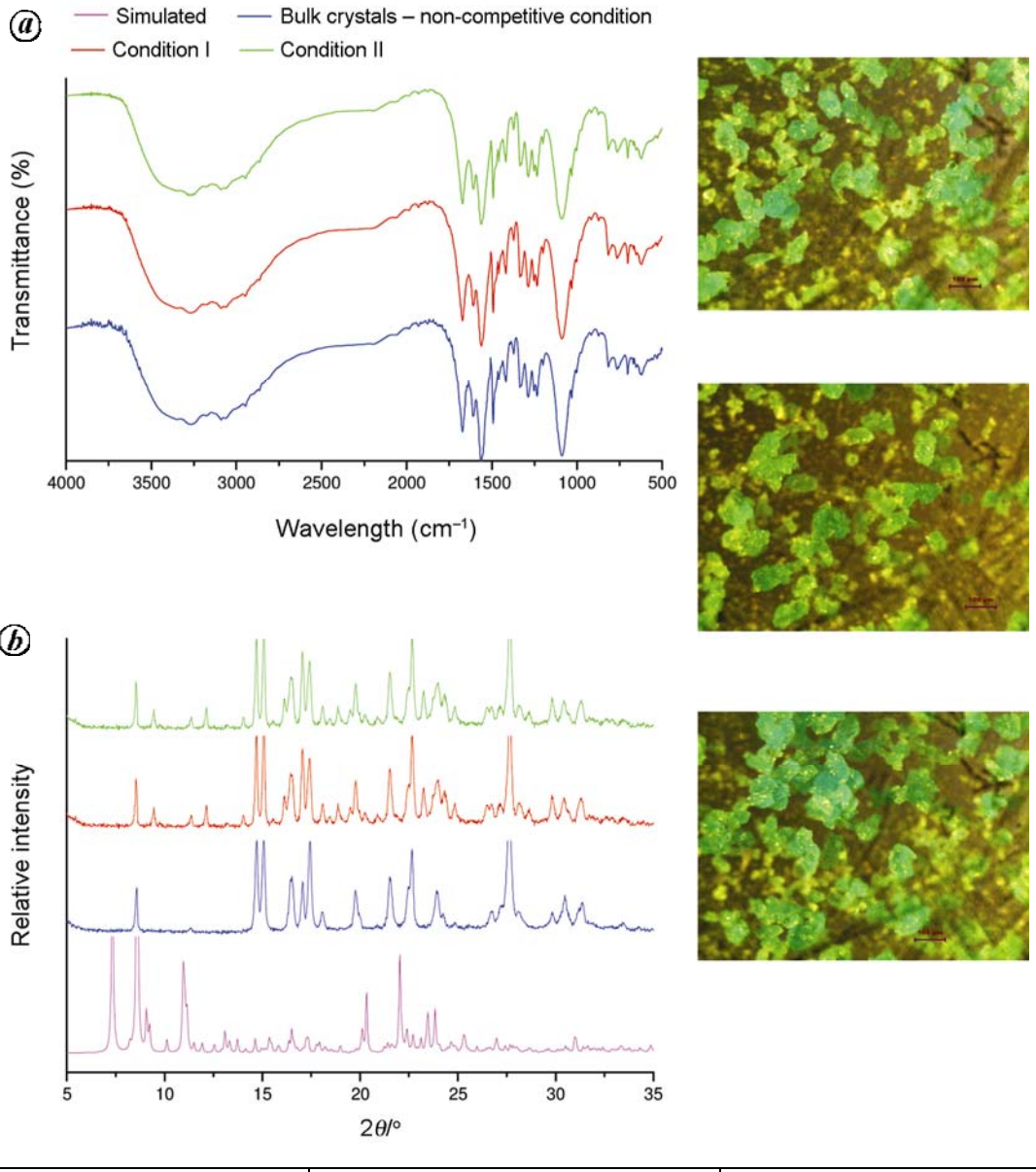

(c)

Non-competitive condition	Condition I	Condition II
Calculated for $C_{48}H_{68}N_{18}O_{18}Cu_2S_2{\cdot}19H_2O$(%): C, 33.54; H, 6.22; N, 14.67 Found: C, 33.13; H, 5.97; N, 14.01	Calculated for $C_{48}H_{68}N_{18}O_{18}Cu_2S_2{\cdot}19H_2O$(%): C, 33.54; H, 6.22; N, 14.67 Found: C, 32.90; H, 6.26; N, 13.97	Calculated for $C_{48}H_{68}N_{18}O_{18}Cu_2S_2{\cdot}19H_2O$(%): C, 33.54; H, 6.22; N, 14.67 Found: C, 33.56; H, 5.85; N, 14.67

Figure 7. FTIR (***a***), XRPD comparison plots (***b***) and elemental analysis data (***c***) obtained for compound **3** under various conditions. Optical micrographs of crystals obtained under non-competitive condition, condition I and condition II respectively (right panel, top to bottom).

series[16], which most often refers to the order of anions in the order of decreasing anion hydration energy or charge density. Thus, it is normally difficult to achieve selective separation of SO_4^{2-} from a complex mixture of other anions. In the present method, however, a phase separation takes place in the form of crystallization. Even then, to have SO_4^{2-} anion separated from a complex mixture of anions containing especially NO_3^- and ClO_4^-, for which the hydration energies are much less compared to those of SO_4^{2-} in the so-called Hofmeister series is remarkable.

Metallogelation

A systematic study of gelation was carried out by reacting **L1**–**L3** with $CuSO_4$ in separate experiments in various aqueous solvents. From the experimental results, it was observed that only **L3** formed a gel when it reacted with $CuSO_4$ under various conditions (Table 2). In other two cases (**L1** and **L2**), precipitates were obtained under various conditions. Gel formation was identified by tube inversion test and further characterized by FESEM, rheology, FTIR and XRPD.

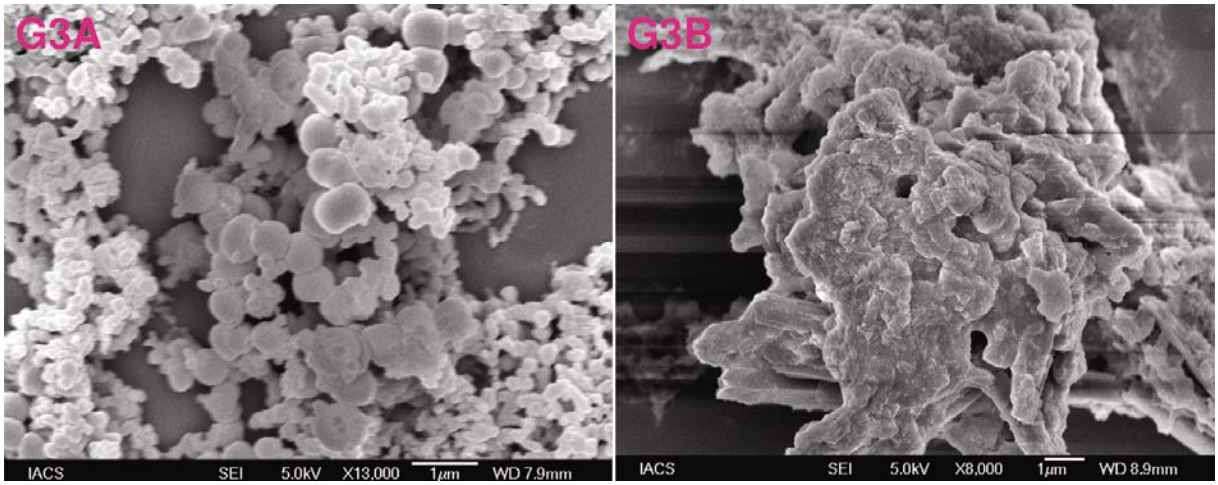

Figure 8. Field emission scanning electron micrographs of xerogels obtained from the gels **G3A** and **G3B**.

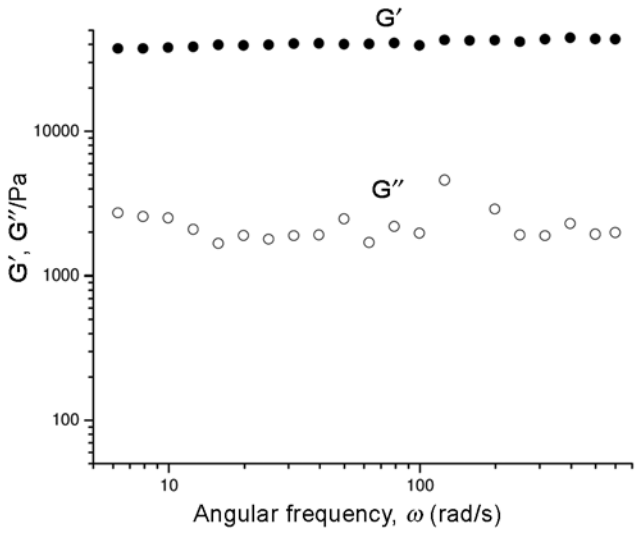

Figure 9. The rheological response of **G3**.

The gels (**G3A** and **G3B**) were not thermo-reversible, indicating coordination polymeric nature of the gel network. The gels were stable under ambient conditions for more than a week. When broken by mechanical shaking and kept overnight undisturbed, they again formed a gel. Thus, both **G3A** and **G3B** displayed thixotropic property.

Microscopy

Microscopic observation of the xerogels under FESEM revealed the presence of globular agglomerates and giant agglomerates in **G3A** and **G3B** respectively (Figure 8).

Rheology

Rheological response of one selected gel **G3B** using dynamic rheology was tested. **G3B** displayed typical gel-like rheological response. Note that elastic modulas **G′** is independent of frequency and considerably higher than loss modulas **G″** over the range of frequencies (Figure 9).

Thus, tube inversion, FESEM and rheology data clearly indicated that **G3A** and **G3B** were indeed gels.

Conclusion

In summary, we have exploited three bis-pyridyl-bis-urea ligands (**L1–L3**) in order to study the effect of the number of carbon atoms on the aliphatic backbone, conformation-dependent ligating topology and multiple hydrogen-bonding (bis-amide) backbones of the ligands on the supramolecular structures and their properties, such anion separation and metallogelation. The flexible aliphatic backbone of **L1** and **L3** played a crucial role in the resultant structures of the CPs. Two different conformations were found in **L1** and **L3** (*syn–syn–syn* and *syn–anti–syn*) in both the crystal structures of **1** and **3** respectively, whereas **L2** exhibited *syn–syn–syn* conformation in **2**. CPs **1**, **2a** and **3** displayed 1D distorted ladder, 1D zigzag and 1D staircase-like topology respectively, in their corresponding crystal structures. Interestingly, all the synthesized CPs **1**–**3** displayed selective sulphate separation from a complex mixture of SO_4^{2-}, NO_3^-, ClO_4^- and $CF_3SO_3^-$ by following an *in situ* CP crystallization technique, indicating that the aliphatic backbone of the ligands did not play a major role in anion separation; the extensive hydrogen bonding involving urea moieties and SO_4^{2-} as observed in the corresponding crystal structures appears to be dictating the selective SO_4^{2-} separation properties of these ligands in the form of the corresponding CPs. Finally, only **L3** exhibited metallogelation property when reacted with $CuSO_4$ in DMF/H_2O and DMSO/H_2O. This could be due to the fact that a right balance between the hydrophobicity and hydrophilicity has been achieved

in **L3** because of the larger number of methylene moieties in the ligand backbone compared to the other ligands in the analogous series. Thus the present study clearly demonstrates the exploitation of supramolecular approach in developing new materials having multiple functional properties, namely anion separation and metallogelation.

1. Janiak, C. and Vieth, J. K., MOFs, MILs and more: Concepts, properties and applications for porous coordination networks. *New J. Chem.*, 2010, **46**(43), 2366–2388.
2. James, S. L., Metal–organic frameworks. *Chem. Soc. Rev.*, 2003, **32**, 276–288.
3. Custelcean, R. and Moyer, B. A., Anion separation with metal–organic frameworks. *Eur. J. Inorg. Chem.*, 2007, 1321.
4. Lumetta, G. J., The problem with anions in the DOE complex. In *Fundamental and Applications of Anion Separations* (eds Moyer, B. A. and Singh, R. P.), Kluwer Academic, New York, 2004, pp. 107–114.
5. Adarsh, N. N., Krishna Kumar, D., Suresh, E. and Dastidar, P., Coordination polymers derived from a bis-pyridyl-bisamide ligand: supramolecular structural diversities and anion binding properties. *Inorg. Chim. Acta*, 2010, **363**, 1367–1376.
6. Desiraju, G. R., *Angew. Chem., Int. Ed. Engl.*, 1995, **34**, 2311; Desiraju, G. R., Crystal engineering: a holistic view. *Angew. Chem., Int. Ed. Engl*., 2007, **46**, 8342–8356.
7. Krishna Kumar, D., Das, A. and Dastidar, P., Remarkably stable porous assembly of nanorods derived from a simple metal–organic framework. *Cryst. Growth Des*., 2007, **7**, 205–207.
8. Carlucci, L., Ciani, G. and Proserpio, D. M., Borromean links and other non-conventional links in 'polycatenated' coordination polymers: re-examination of some puzzling networks. *CrystEngComm.*, 2003, **5**, 269–279.
9. Adarsh, N. N. and Dastidar, P., A Borromean weave coordination polymer sustained by urea–sulphate hydrogen bonding and its selective anion separation properties. *Cryst. Growth Des*., 2010, **10**, 483–487.
10. Dastidar, P., Supramolecular gelling agents: can they be designed? *Chem. Soc. Rev*., 2008, **37**, 2699–2715.
11. Piepenbrock, M.-O. M., Lloyd, G. O., Clarke, N. and Steed, J. W., Metal- and anion-binding supramolecular gels. *Chem. Rev*., 2010, **110**, 1960.
12. Adarsh, N. N., Krishna Kumar, D. and Dastidar, P., Zn(II) metal–organic frameworks (MOFs) derived from a bispyridyl-bisurea ligand: effects of crystallization solvents on the structures and anion binding properties. *CrystEngComm.*, 2008, **10**, 1565–1573.
13. Custelcean, R., Sellin, V. and Moyer, B. A., Sulphate separation by selective crystallization of a urea-functionalized metal–organic framework. *Chem. Commun*., 2007, 1541–1543.
14. Byrne, P., Turner, D. R., Lloyd, G. O., Clarke, N. and Steed, J. W., Gradual transition from N–H···pyridyl hydrogen bonding to the N–H···O tape synthon in pyridyl ureas. *Cryst. Growth Des*., 2008, **8**, 3335–3344.
15. Hofmeister, F., About the science of the effect of salts. *Arch. Exp. Pathol. Pharmakol*., 1888, **24**, 247.
16. Van der Sluis, P. and Spek, A. L., BYPASS: an effective method for the refinement of crystal structures containing disordered solvent regions. *Acta Crystallogr*., *Sect. A*, 1990, **46**, 194.
17. Blatov, V. A. and Proserpio, D. M., TOPOS 4.0, a program package for multipurpose crystallochemical analysis; http://www.topos.ssu.samara.ru/

ACKNOWLEDGEMENTS. We thank DST, New Delhi for financial support. N.N.A. thanks the Indian Association for the Cultivation of Science (IACS), Kolkata for research fellowship. Single crystal X-ray diffraction data were collected at Central Salt and Marine Chemicals Research Institute (CSMCRI), Bhavnagar and the DST-funded National Single Crystal Diffractometer Facility at the Department of Inorganic Chemistry, IACS.